Differences in rates of radiation-induced true and false rib fractures after stereotactic body radiation therapy for Stage I primary lung cancer

Hideharu MIURA*, Toshihiko INOUE, Hiroya SHIOMI and Ryoong-Jin OH

Miyakojima IGRT Clinic, 1-16-22 Miyakojima Hondori, Miyakojima-ku, Osaka, 534-0021, Japan
*Corresponding author: Miyakojima IGRT Clinic, 1-16-22 Miyakojima Hondori, Miyakojima-ku, Osaka, 534-0021, Japan.
Tel: +81-6-6923-3501; Fax: +81-6-6923-3520; Email: hide-miura@osaka-igrt.or.jp

The purpose of this study was to analyze the dosimetry and investigate the clinical outcomes of radiation-induced rib fractures (RIRFs) after stereotactic body radiotherapy (SBRT). A total of 126 patients with Stage I primary lung cancer treated with SBRT, who had undergone follow-up computed tomography (CT) at least 12 months after SBRT and who had no previous overlapping radiation exposure were included in the study. We used the Mantel–Haenszel method and multiple logistic regression analysis to compare risk factors. We analyzed $D(0.5 \text{ cm}^3)$ (minimum absolute dose received by a 0.5-cm^3 volume) and identified each rib that received a biologically effective dose (BED) (BED3, using the linear–quadratic (LQ) formulation assuming an $\alpha/\beta = 3$) of at least 50 Gy. Of the 126 patients, 46 (37%) suffered a total of 77 RIRFs. The median interval from SBRT to RIRF detection was 15 months (range, 3–56 months). The 3-year cumulative probabilities were 45% (95% CI, 34–56%) and 3% (95% CI, 0–6%), for Grades 1 and 2 RIRFs, respectively. Multivariate analysis showed that tumor location was a statistically significant risk factor for the development of Grade 1 RIRFs. Of the 77 RIRFs, 71 (92%) developed in the true ribs (ribs 1–7), and the remaining six developed in the false ribs (ribs 8–12). The BED3 associated with 10% and 50% probabilities of RIRF were 55 and 210 Gy to the true ribs and 240 and 260 Gy to the false ribs. We conclude that RIRFs develop more frequently in true ribs than in false ribs.

Keywords: radiation-induced rib fractures; stereotactic body radiotherapy; lung cancer; dose–response relationship; true and false ribs

INTRODUCTION

Stereotactic body radiotherapy (SBRT) is a highly effective treatment for early-stage primary lung cancer. Local control rate is more than 80–90% in most series, and the 5-year survival rate is better than that reported with conventional radiotherapy, and may be equivalent to that of surgery [1]. Dose escalation is an important means of increasing the effect of radiotherapy and thereby of improving tumor control [2]. Dose escalation to the tumor also increases the dose to neighboring normal tissue. In general, the severity and incidence of acute and late radiation toxicities after SBRT is low [3]. Several studies have reported complications related to SBRT for lung cancer, including chest wall injuries such as radiation-induced rib fractures (RIRFs) [4–10]. To our knowledge, reports of RIRFs as a function of the dose–volume for SBRT and rib location are lacking. Previous analyses have not considered differences in doses to and fractures of the 'true' ribs (ribs 1–7, which articulate with the sternum) and 'false' ribs (ribs 8–12, which do not).

The purpose of this study was to analyze the dosimetry and investigate the clinical outcomes of RIRFs after SBRT, focusing on the effect of rib anatomy.

MATERIALS AND METHODS

The institutional review board approved the study protocol, including the chart review. We obtained written informed consent from each patient. Between July 2007 and December 2012, 184 patients with Stage I primary lung cancer were treated with SBRT. Inclusion criteria for the present study were availability of follow-up chest computed tomography (CT) images at least 12 months after SBRT, and no previous overlapping radiation exposure. Exclusion criteria were traumatic and malignant fractures by hearing patient life style; 58 patient were excluded for meeting these criteria.

The study included 95 men and 31 women with a median age of 76 years (range, 55–98 years). Of these, 82 patients (65%) had primary tumor sites in the upper or middle lobes, and 44 had them in the lower lobes. Stage IA disease was present in 99 patients and Stage IB disease in 27. Only 81 cases were histologically proven; the remaining 45 cases lacked histological proof as a result of age, location of the tumor, and complications such as high-grade chronic obstructive pulmonary disease (COPD) preventing biopsy. The most common histological type among the biopsied patients was adenocarcinoma (40%), followed by squamous cell carcinoma (18%), other histology (6%) and unknown (36%). Of the 126 patients, 64 were classified as ECOG performance status (PS) 0, 41 as PS-1, 12 as PS-2, 8 as PS-3, and 1 as PS-4. More than half the patients (56%) had multiple cancers: 44 had two, 14 had three, nine had four, two had five and one had six. Of the 113 sites of multiple cancers, 41 (36%) were the lung; 11 were the prostate and large intestine (each); 10 were the stomach; nine were the head and neck; eight were the liver; seven were the kidney; three were the urinary bladder, esophagus, breast, and malignant lymphoma (each); and 1 was the gall bladder, small intestine, uterine cervix, and thymus (each). When patients without histological proof had multiple cancers, the primary or metastatic nature of the lung lesions was determined by clinical and imaging factors. Of the lung primaries included in the study, 46 involved the left lung, and 80 involved the right lung.

Treatment procedure

Treatment planning and characteristics have been described previously [11–13]. In brief, treatment planning was done using commercial software (BrainSCAN ver. 5.31® [used July 2007 to September 2010], and iPlan RT image® ver. 4.1.1 or 4.1.2 [used October 2010 to December 2012] planning system; BrainLAB AG[TM], Feldkirchen, Germany). We used immobilization devices as needed (Vac-Lok cushions® and HipFix Thermoplastics®, CIVCO Medical Solutions[TM], Kalona IA, USA). A commercial positioning device (ExacTrac X-ray positioning system® and 6-axis Robotic® couch, BrainLAB[TM]) was used for fine localization. Respiratory motion was suppressed using the Air-bag System[TM] (Niigata Megatoronics Co. Ltd[TM], Niigata, Japan) during the acquisition of treatment-planning 2.5-mm thick CT images (4-slice Brightspeed QX/i®, GE Medical Systems[TM], Waukesha WI, USA) and during SBRT. From July 2007 to September 2010 we performed dose calculation with the Pencil Beam (PB) algorithm (BrainSCAN), which was replaced by the Monte Carlo (MC) algorithm (iPlan RT) from October 2010 to December 2012 to better correct for tissue heterogeneity. Dose calculation was performed with a grid size of 2 mm. Using the PB algorithm, we defined the prescribed dose to the PTV D95 = 100% (48 Gy in 4 fractions). Using the MC algorithm, we defined the prescribed

dose to the GTV D99 = 100% (44 Gy in 4 fractions) [12]. Our previous report showed that a D95 to the PTV of 48 Gy using the PB algorithm was equivalent to a D95 to the PTV of 40 Gy and a D99 to the GTV of 44 Gy using the MC algorithm [12]. The dose fractionation schedules were based on tumor size and proximity to critical structures. The most common dose fractionation was 48 Gy in 4 fractions ($n = 62$), followed by 44 Gy in 4 fractions ($n = 39$). The other fractionation patterns were as follows: 11 patients received 60 Gy in 10 fractions; 7 received 50 Gy in 5 fractions; 2 received 54 Gy in 9 fractions; and 1 each received 56 Gy in 7 fractions, 60 Gy in 8 fractions, 58.5 Gy in 9 fractions, 70 Gy in 14 fractions, and 60 Gy in 12 fractions.

Follow-up and data analysis

We asked all patients to visit our clinic every three months after SBRT. Follow-up CT scans were acquired at each visit using the same CT scanner set at 120 kVp, 1.25-mm slice thickness, tube rotation time 0.5 s and pitch 1.5. An automatic exposure control determined tube currents (range, 50–300 mA). We measured the time to initial appearance of rib fractures from the first day of SBRT. We used the follow-up CT scans on the bone window setting to detect rib fractures, defining RIRF as a disruption of cortical continuity. We checked the follow-up CT scans for fractures anywhere in any rib, regardless of distance from the lesion, and assessed clinical symptoms associated with RIRFs by reviewing the clinical records and grading them using the National Cancer Institute Common Terminology Criteria for Adverse Events ver. 4.0 (NCI–CTCAE) [14]. The probabilities of RIRFs were calculated using the Kaplan–Meier method. The Mantel–Haenszel method and multiple logistic regression analysis were used for uni- and multivariate analyses to compare risk factors (age, treatment year, gender, stage, histology, multiple cancer, performance status, laterality, and target location).

We assessed D(0.5 cm^3) (minimum absolute dose received by a 0.5-cm^3 volume) to the rib, because Taremi *et al.* reported that D(0.5 cm^3) was the dosimetric parameter with the highest correlation with rib fracture [9]. The linear–quadratic (LQ) model was used to account for the fractionation effects of the different schemes being compared. We calculated the biologically effective dose (BED) with an α/β ratio of 3 Gy in each case. We performed dose–volume relationship analyses on all ribs (282 in total) receiving a BED3 of 50 Gy or more [8]. Due to a medially or centrally located target, six patients received significantly less than 50 Gy as BED3 to all ribs. We used logistic regression to predict the probability of occurrence of rib fracture by independent variable of D(0.5 cm^3), performing all statistical analyses using commercial software (SPSS ver. 19.0® IBM[TM], Chicago IL, USA). The log–rank test was also used to determine the significance of differences in cumulative incidence of RIRFs between true and false ribs.
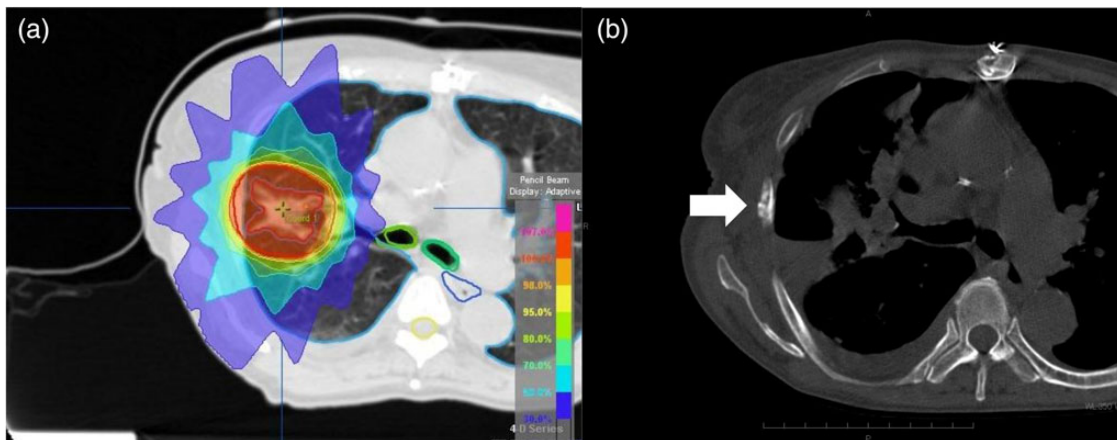
Fig. 1. (**a**) Dose distribution image shows the D (0.5 cm^3) prescribed dose to the rib as 49.6 Gy, with a BED3 of 254.6 Gy. (**b**) Bone window image shows a rib fracture (white arrow) 21 months after completion of SBRT.

RESULTS

Figure 1 shows representative axial dose distributions and images for one RIRF patient. The 3-year cumulative probabilities of Grades 1 and 2 RIRFs were 45% (95% CI, 34–56%) and 3% (95% CI, 0–6%), respectively (Fig. 2). Almost all RIRFs were symptom-free and of NCI–CTCAE Grade 1; they were unexpectedly detected during the follow-up CT. Only three patients had Grade 2 RIRFs they reported a history of accidental thoracic trauma to existing symptom-free Grade 1 rib fractures. No patients had Grade 3 or higher RIRF symptoms.

Uni- and multivariate analyses showed that the target location was a statistically significant risk factor for the development of Grade 1 RIRF. The odds ratio for target location was 0.2823 (95% CI, 0.1086–0.7337; $P = 0.0094$). Patients with primary lesions in the upper and middle lobes had a higher incidence of RIRFs (46%); only 8 (19%) of the 43 patients with lower lobe lesions developed RIRFs (Table 1).

Of the 126 patients, 46 (37%) had 77 RIRFs. Of the 77 RIRFs, 71 (92%) developed in the true ribs, and the remaining 6 (8%) developed in the false ribs. Based on 282 analyzed ribs, true rib fractures occurred in 31% (71/231) of ribs, and false rib fractures occurred in 12% (6/51) (Fig. 3). The median time from SBRT to RIRF detection was 15 months (range, 3–56 months; Table 2) with a median follow-up of 30 months (range: 12–78 months). Of the 46 patients with rib fractures, 22 had fractured 1 rib, 18 had fractured 2, 5 had fractured 3, and 1 had fractured 4 ribs. In all cases of multiple rib fractures, neighboring ribs were involved. In some patients, the number of RIRFs increased over the follow-up period.

The overall incidence of RIRFs in the 282 ribs receiving a BED3 of 50 Gy or more was 27% (77/282). We found, for the D(0.5 cm^3) to a rib, the BED3 giving rise to a 10% and 50% probability of fracture were 76 and 256 Gy, respectively. When subdivided into true and false ribs, the BED3 giving
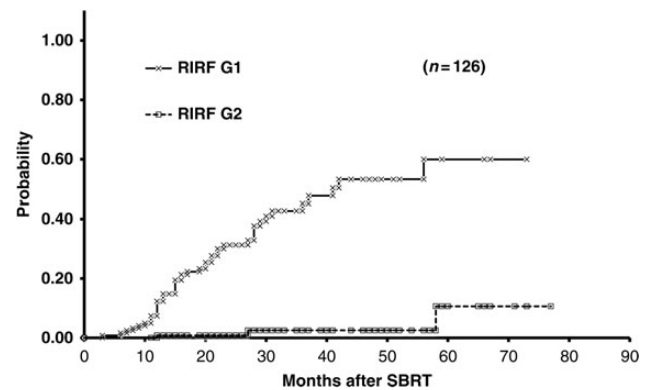

Fig. 2. Cumulative probability of RIRFs after SBRT by symptom grade (NCI–CTCAE). The 3-year cumulative probabilities were 45% and 3% for Grade 1 and 2 RIRFs, respectively.

rise to a 10% and 50% probability of RIRF were 55 and 210 Gy to the true ribs and 240 and 260 Gy to the false ribs, respectively (Fig. 4). This difference was significant by the log–rank test ($P = 0.009$).

DISCUSSION

According to the literature, the incidence of RIRFs after SBRT for lung cancers varies from 21–41%, and the actuarial risk ranges between 27% and 45% [4–9]. This wide variation may be attributable to patient selection and the dose threshold used. The treatment technique and dose fractionation, outcome measures, and follow-up procedures also differ widely among institutions. The median time from SBRT to initial RIRF detection, which was sometimes difficult to determine because of unclear clinical findings, generally ranged from 15–22 months in these previous studies (Table 2).

Table 1.   Uni- and multivariate analyses for Grade 1 RIRFs

Item	Category	G1 RIRF (−)	G1 RIRF (+)	No. patients	Univariate analysis Chi-square	Univariate analysis P-value	Multivariate analysis Odds Ratio	95% C.I.		Multivariate analysis P-value
Age	~76	44	21	65	1.0219	0.3121	1.2380	0.5429	2.8230	0.6118
	77~	36	25	61						
Period	~2010.9	45	35	80	4.9582	0.0260*	0.5409	0.2187	1.3377	0.1835
	2010.10~	35	11	46						
Gender	Male	63	32	95	1.3282	0.2491	1.4288	0.5536	3.6877	0.4608
	Female	17	14	31						
Stage	IA	66	33	99	2.0087	0.1564	1.8488	0.6774	5.0457	0.2303
	IB	14	13	27						
Histology	NSCLC	46	35	81	4.3948	0.0360*	0.6364	0.2523	1.6054	0.3384
	No Proof	34	11	45						
Multiple Cancer	Absent	33	23	56	0.9056	0.3413	0.6594	0.2887	1.5061	0.3231
	Present	47	23	70						
PS	0~1	70	35	105	2.7391	0.0979	2.1358	0.7179	6.3545	0.1725
	2~4	10	11	21						
Laterality	Left	26	20	46	1.5186	0.2178	0.7349	0.3184	1.6960	0.4704
	Right	54	26	80						
Target Location	Upper/Middle	45	38	83	9.0265	0.0027**	0.2823	0.1086	0.7337	0.0094*
	Lower	35	8	43						
Total		80	46	126						

G1 = Grade 1, RIRF = radiation-induced rib fracture, NSCLC = non–small cell lung cancer, PS = performance status. Significant difference *$P < 0.05$, **$P < 0.01$.
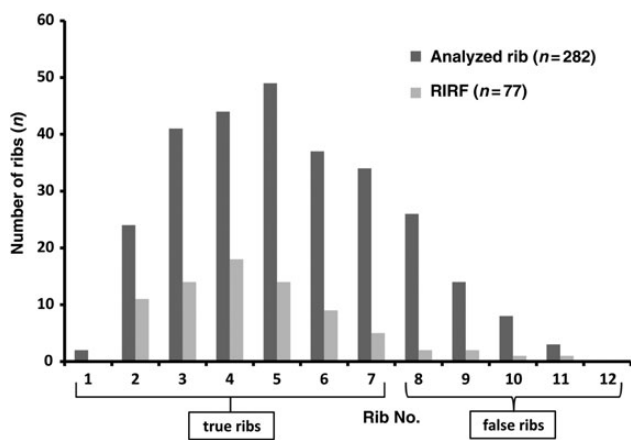

Fig. 3. Distribution of analyzed ribs and radiation-induced rib fractures (RIRFs) for each rib. Of the 126 patients, 46 (37%) had 77 RIRFs, of which 71 (92%) developed in the true ribs (ribs 1–7), and the remaining six (8%) developed in the false ribs (ribs 8–12).

Some studies have cited gender as an independent risk factor for RIRF after SBRT for lung cancer [4, 6, 8]. They estimated that postmenopausal women had a high risk of osteoporosis, with an accompanying high risk of RIRF. However, we did not recognize gender as a risk factor. One reason for this could be that our study included older patients (median age, 76 years; range, 55–98 years). Therefore, the risk factor of age may have superseded the one of gender. We previously reported significant differences between the characteristics of primary and metastatic lung cancer patients treated with SBRT at our institution, including age; patients with primary lung cancers were older than those with metastatic tumors [11].

Another RIRF risk factor described previously is distance from the rib to the tumor (varying from <1.6–2.0 cm) [4, 7, 8]. However, it had not been demonstrated whether these data have scientific validity. Evaluation of distance from tumor to rib is not appropriate, because intensity-modulated radiation therapy (IMRT) and volumetric-modulated arc therapy (VMAT) techniques can decrease dose to the organ at risk (OAR), such as ribs. The multivariate analysis in our study showed that the target location was a statistically significant risk factor for the development of RIRFs. Of the 77 RIRFs, 71 (92%) developed in the true ribs, and the remaining 6 developed in the false ribs. To our knowledge, differences in

Table 2. Incidence of RIRFs and median time from SBRT to RIRF detection

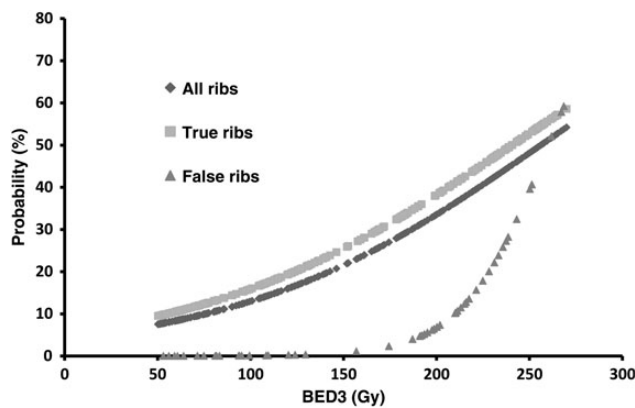| Author (year)	No. patients	Incidence	Actuarial risk	Median months
Pettersson *et al.* (2009) [5]	33	7/33 (21%)	NA	15 (8–38)
Nambu *et al.* (2011) [8]	177	41/131 (31%)	27.4% (2-year)	21 (4–58)
Kim *et al.* (2013) [6]	118	48/118 (41%)	42.4% (2-year)	17 (4–52)
Asai *et al.* (2012) [7]	116	28/116 (24%)	37.7% (3-year)	22 (9–42)
Taremi *et al.* (2012) [9]	46	17/46 (37%)	38% (2-year)	21 (7–40)
Present study	126	46/126 (37%)	45% (3-year)	15 (3–56)

Fig. 4. Dose–response functions for rib fractures, grouped by all ribs, the true ribs, and the false ribs. The BED3 associated with a 10% and 50% probability of RIRF were 55 and 210 Gy to the true ribs, and 240 and 260 Gy to the false ribs, respectively.

the incidence of RIRFs between true and false ribs have not been clearly described in previous studies.

Because Emami's classic paper regarding the tolerance of normal tissue did not seem appropriate to advanced precision radiotherapy [15], Marks *et al.* proposed a new Quantitative Analysis of Normal Tissue Effects in the Clinic (QUANTEC) model [16] to help predict clinical outcomes. However, they could not propose a model specific to rib fractures because of the lack of clinical data and appropriate dosimetric parameters regarding RIRFs after SBRT or IMRT with a steep dose gradient administered to the affected ribs. Therefore, further information was necessary to establish the risk levels for RIRFs.

Pettersson *et al.* concluded that the risk of RIRF following hypofractionated SBRT was related to the dose administered to 2 cm^3 of the rib, which is a dose–volume-histogram parameter [5]. Taremi *et al.* reported that D(0.5 cm^3) was the dosimetric parameter with the highest correlation with rib fracture and presented an illustration showing the anatomic locations of 41 fractured ribs in 17 patients with radiation-induced bone injury. Their figure showed 30 (73%) true rib fractures (excluding the first rib), and 11 (23%) false rib

fractures (excluding the 12th rib) [9]. However, they did not recognize the anatomical characteristics of true and false ribs.

In our study, the BED3 associated with 10% and 50% probabilities of RIRF were 55 and 210 Gy to the true ribs and 240 and 260 Gy to the false ribs, respectively. The probability of RIRF was significantly different for true and false ribs, especially in lower doses to the rib. The difference in the probability of RIRFs between true and false ribs reduced with increasing dose to the rib.

A possible reason that fractures of false ribs are less common than fractures of true ribs is rib positions, length and flexibility. The number of analyzed false ribs is low, because the 11th and 12th ribs are not situated over lung parenchyma. Rib length increases from ribs 1 to 7, and decreases from ribs 8 to 12, with ribs 11 and 12 being shorter than any true rib. True ribs may be more likely to break because of the decreased flexibility caused by their being anchored at the costovertebral and sternocostal junctions. Rib fractures can be caused by the force of a patient's own muscles in instances such as severe coughing, twisting, and sports such as tennis and rugby. Since a stronger force is needed to fracture false ribs, similarly, a substantially higher SBRT dose is needed to cause RIRFs in false ribs. The location of the rib and the dose it receives are an important factor in RIRFs. Thus, a new dose–response concept recognizing the different risk to true and false ribs would likely be required.

Some factors that will add some uncertainty to the probability of fracture for each rib can be seen on the dose–volume histogram, LQ model, calculation algorithm, and breathing-related organ motion. The main issue is whether cell survival curves, in addition to LQ properties at doses per fraction delivered in standard fractionated radiation therapy, exhibit linear behavior at the larger doses per fraction delivered in hypofractionated radiation therapy [17]. Using PB and MC calculations, in general, there were significant dose differences to lung cancers with inhomogeneous density [13]. Abdominal compression with the Air Bag–system reduces movement of the diaphragm, which can decrease intrathoracic organ motion [12].

Although factors that can reduce rib dose relate to chest wall involvement by the tumor, a T1 lung cancer is unlikely to seed the entire pleural space without breaching the pleura [18]. IMRT, VMAT, and image-guided radiotherapy (IGRT) techniques can play an important role in reducing rib dose when the tumor is close to the chest wall [19]. 4D-IGRT with pre-treatment verification of the target position and online correction of errors can reduce safety margins effectively in pulmonary SBRT [20], but this must be done with care [21].

Although the incidence of RIRFs was high in our study, patients experienced little morbidity. We considered the treatment to be well tolerated because no severe adverse effects were observed. SBRT is a safe and effective treatment option for patients with early-stage lung cancer. RIRFs typically occur later, with a median time of onset of greater than 17 months after SBRT [6, 7, 9]. Most patients' RIRFs were asymptomatic. Grade 1 symptoms advanced to Grade 2 only through exacerbation of an existing RIRF from mechanical trauma. Patient education about fall prevention and avoidance of torso-twisting motions may help to lower the incidence of Grade 2 symptoms. Therefore, screening for and prevention of asymptomatic rib fractures may be clinically important.

In conclusion, target location adjacent to the true ribs is a statistically significant risk factor for the development of Grade 1 RIRFs after SBRT. RIRFs developed more frequently in the true ribs than in the false ribs. The BED3 associated with a 10% and 50% probability of RIRF were 55 and 210 Gy to the true ribs and 240 and 260 Gy to the false ribs, respectively. Every effort should be made to decrease rib dose, particularly to the true ribs, in order to reduce the risk of RIRF.

REFERENCES

1. Onishi H, Araki T, Shirato H *et al*. Stereotactic hypofractionated high-dose irradiation for stage I non–small cell lung carcinoma: clinical outcomes in 245 subjects in a Japanese multiinstitutional study. *Cancer* 2004;**101**:1623–31.
2. McGarry RC, Papiez L, Williams M *et al*. Stereotactic body radiation therapy of early-stage non-small-cell lung carcinoma: phase I study. *Int J Radiat Oncol Biol Phys* 2005;**63**:1010–5.
3. Haasbeek CJ, Lagerwaard FJ, Antonisse ME *et al*. Stage I non–small cell lung cancer in patients aged ≥75 years: outcomes after stereotactic radiotherapy. *Cancer* 2010;**116**:406–14.
4. Nambu A, Onishi H, Aoki S *et al*. Rib fracture after stereotactic radiotherapy for primary lung cancer: prevalence, degree of clinical symptoms, and risk factors. *BMC Cancer* 2013;**13**:68.
5. Pettersson N, Nyman J, Johansson KA. Radiation-induced rib fracture after hypofractionated stereotactic body radiation therapy of non–small cell lung cancer: a dose– and volume–response analysis. *Radiother Oncol* 2009;**91**:360–8.
6. Kim SS, Song SY, Kwak J *et al*. Clinical prognostic factors and grading system for rib fracture following stereotactic body radiation therapy (SBRT) in patients with peripheral lung tumors. *Lung Cancer* 2013;**79**:161–6.
7. Asai K, Shioyama Y, Nakamura K *et al*. Radiation-induced rib fractures after hypofractionated stereotactic body radiation therapy: risk factors and dose–volume relationship. *Int J Radiat Oncol Biol Phys* 2012;**84**:768–73.
8. Nambu A, Onishi H, Aoki S *et al*. Rib fracture after stereotactic radiotherapy on follow-up thin-section computed tomography in 177 primary lung cancer patients. *Radiat Oncol* 2011;**6**:137.
9. Taremi M, Hope A, Lindsay P *et al*. Predictors of radiotherapy induced bone injury (RIBI) after stereotactic lung radiotherapy. *Radiat Oncol* 2012;**7**:159.
10. Voroney JP, Hope A, Dahele MR *et al*. Chest wall pain and rib fracture after stereotactic radiotherapy for peripheral non–small cell lung cancer. *J Thorac Oncol* 2009;**4**:1035–7.
11. Inoue T, Oh R-J, Shiomi H *et al*. Stereotactic body radiotherapy for pulmonary metastases. Prognostic factors and adverse respiratory events. *Strahlenther Onkol* 2013;**189**: 285–92.
12. Miura H, Masai N, Oh RJ *et al*. Approach to dose definition of the gross tumor volume for lung cancer with respiratory tumor motion. *J Radiat Res* 2013;**54**:140–5.
13. Miura H, Masai N, Oh RJ *et al*. Clinical introduction of Monte Carlo treatment planning for lung stereotactic body radiotherapy. *J Appl Clin Med Phys* 2014;**15**:38–46.
14. US Department of Health and Human Services, NIH, NCI. Common Terminology Criteria for Adverse Events (CTCAE) ver. 4.0, published: 28 May 2009 (ver. 4.03: 14 June 2010). 17 December 2011. http://www.hrc.govt.nz/sites/default/files/CTCAE%20manual%20-%20DMCC.pdf#search='v4.0CTCAE (6 February 2013, date last accessed).
15. Emami B, Lyman J, Brown A *et al*. Tolerance of normal tissue to therapeutic irradiation. *Int J Radiat Oncol Biol Phys* 1991;**15**:109–22.
16. Marks LB, Yorke ED, Jackson A *et al*. Use of normal tissue complication probability models in the clinic. *Int J Radiat Oncol Biol Phys* 2010;**76**:S10–9.
17. Kirkpatrick JP, Meyer JJ, Marks LB. The linear–quadratic model is inappropriate to model high dose per fraction effects in radiosurgery. *Semin Radiat Oncol* 2008;**18**:240–3.
18. Colby TV, Koss MN, Travis WD. Tumors of the lower respiratory tract. In: Rosai J, Sobin LH (eds). *Atlas of Tumor Pathology. Third Series Fascicle 13*. Washington, DC: AFIP, 1995, 107–34.
19. Ding L, Lo YC, Kadish S *et al*. Volume Modulated Arc Therapy (VMAT) for pulmonary Stereotactic Body Radiotherapy (SBRT) in patients with lesions in close approximation to the chest wall. *Front Oncol* 2013;**22**;3:12.
20. Guckenberger M, Krieger T, Richter A *et al*. Potential of image-guidance, gating and real-time tracking to improve accuracy in pulmonary stereotactic body radiotherapy. *Radiother Oncol* 2009;**91**:288–95.
21. Van Herk M. Will IGRT live up to its promise? *Acta Oncol* 2008;**47**:1186–7.